Phase Behavior of Concentrated Aqueous Solutions of Cetyltrimethylammonium Bromide (CTAB) and Sodium Hydroxy Naphthoate (SHN)

R. Krishnaswamy,† S. K. Ghosh,† S. Lakshmanan,† V. A. Raghunathan,*,† and A. K. Sood‡

Raman Research Institute, Bangalore 560 080, India, and Deparment of Physics, Indian Institute of Science, Bangalore 560 012, India

Received July 2, 2005. In Final Form: August 27, 2005

We have characterized the phase behavior of mixtures of the cationic surfactant cetyltrimethylammonium bromide (CTAB) and the organic salt 3-sodium-2-hydroxy naphthoate (SHN) over a wide range of surfactant concentrations using polarizing optical microscopy and X-ray diffraction. A variety of liquid crystalline phases, such as hexagonal, lamellar with and without curvature defects, and nematic, are observed in these mixtures. At high temperatures the curvature defects in the lamellar phase are annealed gradually on decreasing the water content. However, at lower temperatures these two lamellar structures are separated by an intermediate phase, where the bilayer defects appear to order into a lattice. The ternary phase diagram shows a high degree of symmetry about the line corresponding to equimolar CTAB/SHN composition, as in the case of mixtures of cationic and anionic surfactants.

Introduction

The physical properties of ionic surfactants are very sensitive to the nature of the counterions. In particular, counterions that are embedded in the surfactant micelle are known to dramatically modify the viscoelastic properties of these solutions through the formation of long wormlike micelles.[1−4] One extreme limit of an embedded counterion is an oppositely charged surfactant, and aqueous solutions of such surfactant mixtures are known to show many interesting properties, such as low critical micellar concentration (CMC), high surface activity, formation of liquid crystalline phases at higher water content, and spontaneous formation of vesicles.[5−9]

The cetyltrimethylammonium bromide (CTAB)−water binary system forms an isotropic solution of spherical micelles just above the CMC. On increasing the surfactant concentration the micelles become rodlike. With further addition of surfactant a nematic phase made up of rodlike micelles is observed at room temperature over a narrow concentration range, beyond which a 2D hexagonal phase is seen.[10,11] Addition of organic salts, such as sodium salicylate (SS), transforms the rodlike CTAB micelles into long wormlike micelles, whose rheological properties have been the subject of many theoretical and experimental studies.[3,4] A somewhat similar system that has been well studied is mixtures of CTAB with sodium hydroxy naphthoate (SHN), which exhibits a shear-induced vesicle to micelle transition.[12−16] However, all these investigations have been confined to dilute solutions with surfactant concentrations ≤ 5 wt %. We recently studied the formation of complexes of some anionic polyelectrolytes including DNA with the CTAB−SHN system and observed some novel structures of these complexes.[17] These studies suggest that the structures of these complexes are related to structures formed by the surfactant system at high concentrations. Therefore, to understand the formation of these structures, we have undertaken a detailed study of the phase behavior of concentrated aqueous solutions of CTAB and SHN. Another motivation was the fact that almost all of the earlier studies on similar systems have been confined to low surfactant concentrations.

In this paper we describe the phase behavior of concentrated aqueous solutions of CTAB and SHN for a number of molar ratios (α = [SHN]/[CTAB]), deduced from polarizing microscopy and X-ray diffraction studies. At low α the phase behavior is similar to that of the CTAB−water binary system. With increasing SHN concentration a lamellar phase with curvature defects is found. At lower temperatures (<∼60 °C) this phase transforms into a regular lamellar phase via an intermediate phase on decreasing the water content. At still higher SHN concentration a nematic phase is found. A partial ternary phase diagram has been constructed, which exhibits a high degree of symmetry about the equimolar CTAB/SHN composition, reminiscent of the phase behavior of mixtures of anionic and cationic surfactants.

† Raman Research Institute.
‡ Indian Institute of Science.

(1) Rehage, H.; Hoffmann, H. *J. Phys. Chem.* **1988**, *92*, 4712.
(2) Shikata, T.; Hirata, H.; Kotaka, T. *Langmuir* **1988**, *4*, 354.
(3) Cates, M. E.; Candau, S. J. *J. Phys.: Condens. Matter* **1990** 2, 6869.
(4) Berret, J. F. cond-mat/0406681, 2004.
(5) Lucassen-Reynders, E. H.; Lucassen, J.; Giles, D. *J. Colloid Interface Sci.* **1981**, *81*, 150.
(6) Kaler, E. W.; Herrington, K. L.; Murthy, A. K.; Zasadzinski, J. A. N. *J. Phys. Chem.* **1992**, *96*, 6698.
(7) Yatcilla, M. T.; Herrington, K. L.; Brasher, L. L.; Kaler, E. W. *J. Phys. Chem.* **1996**, *100*, 5874.
(8) Herrington, K. L.; Kaler, E. W.; Millar, D. D.; Zasadzinski, J. A.; Chiruvolu, S. *J. Phys. Chem.* **1993**, *97*, 13792.
(9) Blandamer, M. J.; Briggs, B.; Cullis, P. M.; Engberts, B. F. N. *Phys. Chem. Chem. Phys.* **2000**, *2*, 5146.
(10) Auvray, X.; Petipas, C.; Anthore, R.; Ricco, I.; Lattes, A. *J. Phys. Chem.* **1989**, *93*, 7458.
(11) Coppola, L.; Gianferri, R.; Nicotera, I.; Oliviero, C.; Ranieri, G. A. *Phys. Chem. Chem. Phys.* **2004**, *6*, 2364.
(12) Mishra, B. K.; Samant, S. D.; Pradhan, P.; Mishra, S. B.; Manohar, C. *Langmuir* **1993**, *9*, 894.
(13) Horbaschek, K.; Hoffmann, H.; Thunig, C. *J. Colloid Interface Sci.* **1998**, *206*, 439.
(14) Salkar, R. A.; Hassan, P. A.; Samant, S. D.; Valaulikar, B. S.; Kumar, V. V.; Kern, F.; Candau, S. J.; Manohar, C. *Chem. Commun.* **1996**, *10*, 1223.
(15) Mendes, E.; Narayanan, J.; Oda, R.; Kern, F.; Candau, S. J.; Manohar, C. *J. Phys. Chem. B* **1997**, *10*, 2256.
(16) Mendes, E.; Oda, R.; Manohar, C.; Narayanan, J. *J. Phys. Chem.* **1998**, *102*, 338.
(17) Krishnaswamy, R.; Mitra, P.; Raghunathan, V. A.; Sood, A. K. *Europhys. Lett.* **2003**, *62*, 357.

10.1021/la051781q CCC: $30.25 © 2005 American Chemical Society
Published on Web 10/06/2005

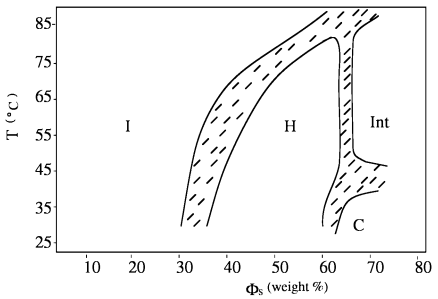

Figure 1. Phase diagram of the CTAB−SHN−water system at α = 0.25. I, H, Int, and C denote the isotropic, hexagonal, intermediate, and crystalline phases, respectively. The shaded regions in this and all subsequent phase diagrams correspond to multiphase regions.

Materials and Methods

Cetyltrimethylammonium bromide (CTAB) and 3-hydroxy-2-naphthoic acid (HNA) were purchased from Aldrich. Sodium-3-hydroxy-2-naphthoate (SHN) was prepared by adding an equivalent amount of an aqueous solution of sodium hydroxide (NaOH) to an ethanol solution of HNA. To prepare the ternary solution, appropriate amounts of CTAB and SHN were first weighed out into a tube. The required concentration of the surfactant solution was obtained by adding deionized water (Millipore). The tube was then sealed and left in an oven at 40 °C for more than 2 weeks. For microscopic observations the samples were taken between a glass slide and a cover slip. Samples were taken in glass capillaries (Hampton Research) for X-ray diffraction studies. Aligned samples in the lamellar phase were obtained by sucking them into thin capillaries of 0.5 mm diameter. One millimeter diameter capillaries were used to obtain unoriented samples. The capillaries were flame-sealed, and the sealed ends were dipped in glue as an additional precaution against loss of water from the sample. A rotating anode generator (Rigaku, UltraX 18) operating at 48 kV and 80 mA was the source of X-rays. Cu Kα radiation (0.154 nm) was selected using a flat graphite monochromator (Huber). Diffraction patterns were collected on an image plate detector (Marresearch). Typical exposure time was 1−2 h.

Results

The phase behavior of the mixtures was studied at a SHN to CTAB molar ratio α = 0.25, 0.43, 0.67, 1.0, 1.5, and 1.85. For each α (CTAB + SHN) concentration (ϕ_s) was varied from 10 to 80 wt %. Microscopy observations were made over a temperature range from 30 to 85 °C. Phases were identified from their characteristic microscopy textures and diffraction patterns. Multiphase regions in the phase diagrams were deduced from coexisting microscopy textures. Around 100 samples were investigated to construct the ternary phase diagram.

Phase Behavior at α = 0.25. A flow-birefringent isotropic viscoelastic gel (I) is observed at low values of ϕ_s (Figure 1). On increasing ϕ_s the samples exhibit the characteristic texture of the hexagonal phase (H) under the microscope (Figure 2). Diffraction patterns of these samples show two peaks in the small-angle region with the corresponding spacings in the ratio $1:1/\sqrt{3}$, confirming the two-dimensional hexagonal structure. The lattice parameter of this phase decreases as ϕ_s is increased (Table 1). For $\phi_s > \sim 65$ a crystalline phase is obtained at room temperature. However, on increasing the temperature another phase (Int) is observed whose texture (Figure 3) is different from that of the other liquid crystalline phases. This phase is found to be much more viscous than the other phases observed in this system. We will refer to this as an intermediate phase for reasons to be discussed later in the paper.

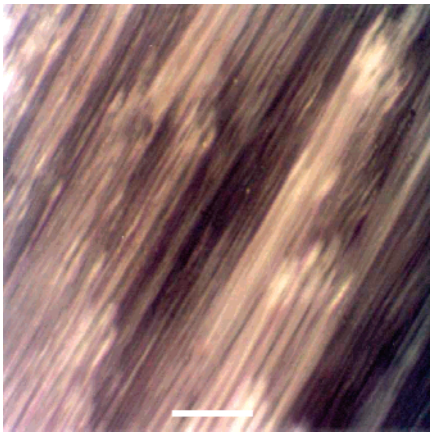

Figure 2. Typical texture of the hexagonal (H) phase of the CTAB−SHN−water system observed under the polarizing microscope. α = 0.25, ϕ_s = 50, T = 30 °C. The scale bar corresponds to 0.1 mm.

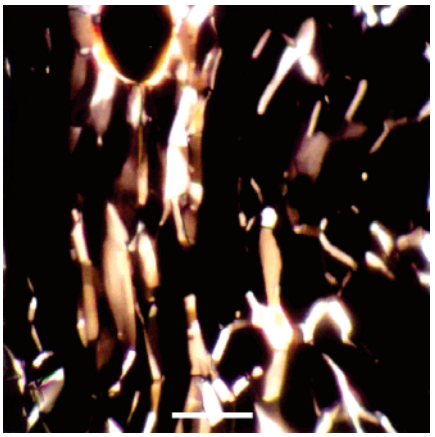

Figure 3. Typical texture of the intermediate phase (Int) observed between crossed polarizers. α = 1.0, ϕ_s = 60, T = 30 °C. Scale bar corresponds to 0.1 mm.

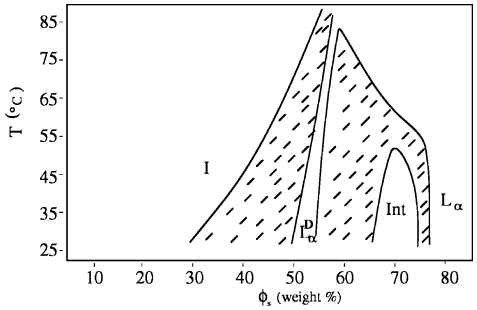

Figure 4. Phase diagram of the CTAB−SHN−water system at α = 0.43. L_α^D and L_α denote lamellar phases with and without curvature defects, respectively.

Table 1. Spacings of the Observed Reflections and Corresponding Values of the Lattice Parameter (*a*) of the Hexagonal (*H*) Phase of the CTAB−SHN−water System at α = 0.25 and *T* = 30 °C

ϕ_s	d_1 (nm)	d_2 (nm)	a (nm)
40	6.13		7.08
50	5.59	3.22	6.45
60	5.12	2.96	5.92

Phase Behavior at α = 0.43, 0.67, 1.0, and 1.5. The phase behavior of the system at these four compositions is qualitatively very similar (Figures 4−7). An isotropic phase is observed at low ϕ_s in all except the equimolar mixture, which transforms into a lamellar (L_α^D) phase at

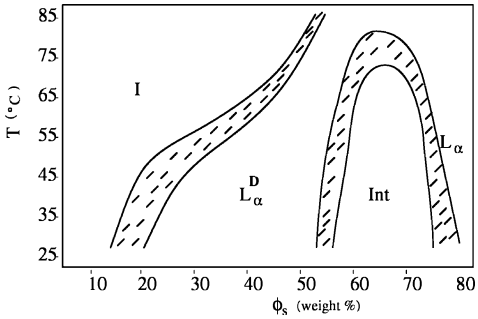

Figure 5. Phase diagram of the CTAB−SHN−water system at α = 0.67.

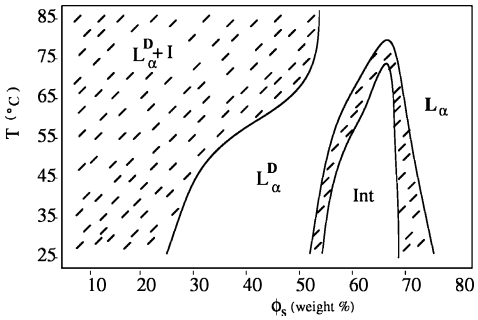

Figure 6. Phase diagram of the CTAB−SHN−water system at α = 1.0.

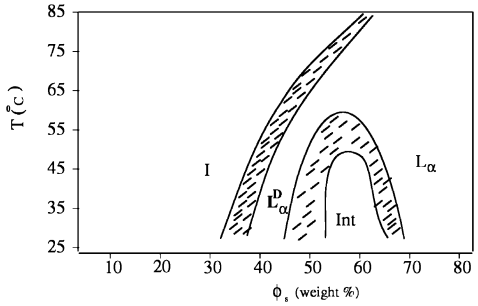

Figure 7. Phase diagram of the CTAB−SHN−water system at α = 1.5.

higher ϕ_s, whose diffraction patterns, to be discussed below, suggest the presence of curvature defects in the bilayers. On increasing the temperature at these concentrations a L_α^D−I transition is observed. The corresponding transition temperature increases strongly with increasing ϕ_s. At α = 1 the L_α^D phase is found to coexist with an isotropic phase at $\phi_s = 10$. At higher concentrations a pure L_α^D is obtained. On increasing ϕ_s further the intermediate phase is obtained at all four compositions, which transforms into L_α^D on heating. At still higher ϕ_s a lamellar (L_α) phase reappears whose diffraction patterns do not show any evidence for defects in the bilayers.

The microscopy textures of the lamellar phase occurring on either side of Int at room temperature are identical (Figure 8). However, as mentioned above, their diffraction patterns differ in one respect. The diffraction pattern of the L_α^D phase present at lower ϕ_s consists of two reflections corresponding to the lamellar periodicity along q_z, z being the direction of the bilayer normal, and a more diffuse reflection along the orthogonal direction $q_\perp$ (Figure 9). The diffuse reflection is absent in the L_α phase occurring at higher ϕ_s (Figure 10). The lamellar periodicity and the position of the diffuse peak in the lamellar phase at α = 1.0 are given in Table 2 as a function of ϕ_s. At high temperatures the diffuse peaks fade away gradually on increasing ϕ_s. On the other hand, at lower temperatures the Int phase intervenes between the two lamellar

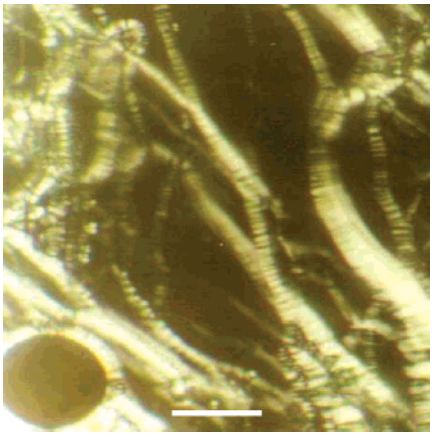

Figure 8. Typical texture of the lamellar (L_α^D) phase under crossed polarizers. α = 1.0, ϕ_s = 50, T = 30 °C. Scale bar represents 0.1 mm.

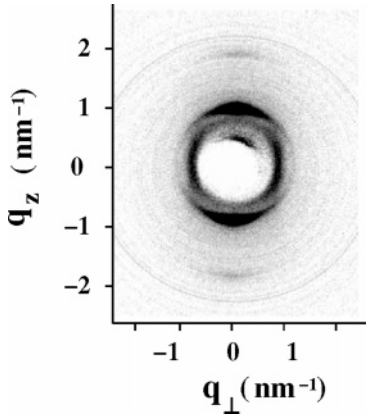

Figure 9. Typical diffraction pattern of the lamellar (L_α^D) phase occurring at intermediate values of ϕ_s (α = 1.0, ϕ_s = 50).

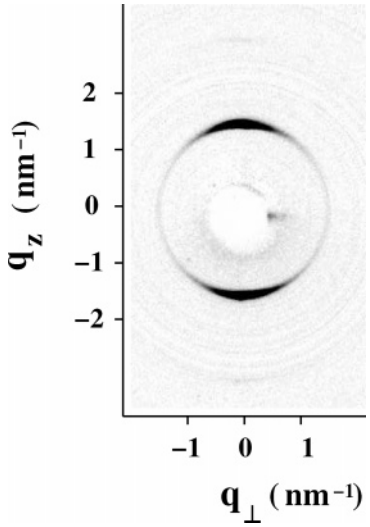

Figure 10. Typical diffraction pattern of the lamellar (L_α) phase occurring at very high values of ϕ_s (α = 1.0, ϕ_s = 80).

structures. This is the reason for referring to this as the intermediate phase. The diffraction pattern of this structure contains many reflections, indicating a high degree of positional order (Figure 11). It does not show any changes even after aging the samples for about 1 year, suggesting thermodynamic stability of this phase.

The I−L_α^D phase boundary first shifts to lower ϕ_s with increasing α, such that at α = 1.0 coexistence of the two phases is seen even at $\phi_s \approx 10$. At much lower ϕ_s (∼1.0), a precipitate which phase separates at the top of the

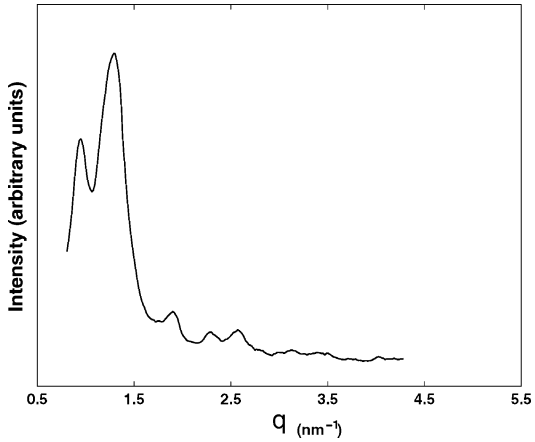

Figure 11. Diffraction pattern of the intermediate (Int) phase ($\alpha = 1$, $\phi_s = 60$).

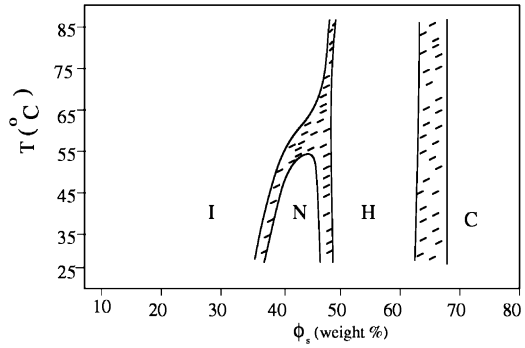

Figure 12. Phase diagram of the CTAB−SHN−water system at $\alpha = 1.85$. N denotes the nematic phase.

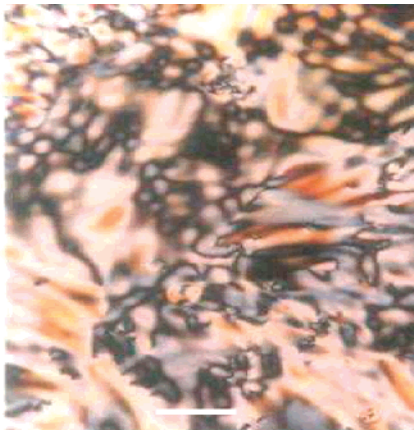

Figure 13. Typical threadlike texture of the nematic (N) phase. $\alpha = 1.85$, $\phi_s = 40$, $T = 30$ °C. Scale bar represents 0.1 mm.

Table 2. Variation of the Lamellar Periodicity d and Spacing of the Diffuse Peak d_d with ϕ_s at $\alpha = 1.0$ and $T = 30$ °C

ϕ_s	d (nm)	d_d (nm)	phase
30	9.60	5.94	L_α^D
40	7.17	6.93	L_α^D
50	5.85	7.45	L_α^D
80	39.8		L_α

solution, is seen at $\alpha \approx 1.0$. When the surfactant concentration is increased the precipitate dissolves and the above-mentioned coexistence of I and L_α^D phases is observed. On increasing α to 1.5 the I−L_α^D boundary moves again to higher values of ϕ_s and the phase diagram is somewhat similar to that at $\alpha = 0.43$. The range of stability of the intermediate phase (both in T and ϕ_s) also shows a maximum at $\alpha \approx 1.0$.

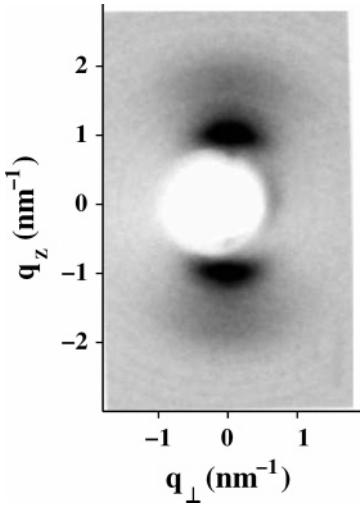

Figure 14. X-ray diffraction pattern of the nematic (N) phase at $\alpha = 1.85$ ($\phi_s = 40$ and $T = 30$ °C).

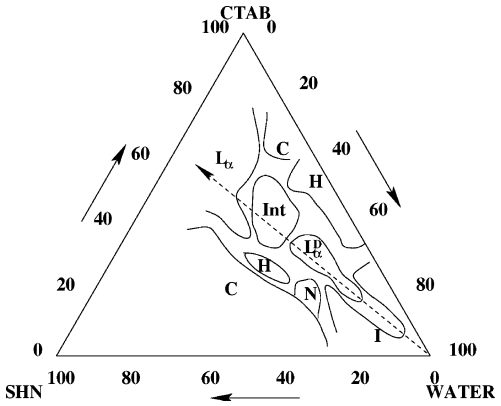

Figure 15. Phase diagram of the CTAB−SHN−water system at 30 °C. The concentrations are in wt %. I, L_α^D, L_α, H, Int, N, and C denote the isotropic, lamellar phase with curvature defects, regular lamellar phase, hexagonal phase, intermediate phase, nematic phase, and crystalline phase, respectively. The dashed line indicates samples with equimolar CTAB/SHN composition.

Phase Behavior at $\alpha = 1.85$. At this SHN concentration the L_α phase disappears. A viscous isotropic phase is obtained for $\phi_s \leq 30$, beyond which a nematic (N) phase appears (Figure 12). The latter phase is also very viscous and exhibits the characteristic threadlike texture under the polarizing microscope (Figure 13). Pseudo-isotropic regions, where the optic axis is normal to the glass plates, were not found in any of the samples studied. Diffraction patterns of this phase show partial alignment, probably due to the shear when the samples were sucked into the capillaries (Figure 14). On increasing ϕ_s the nematic phase transforms into a hexagonal (H) phase, as indicated by both the microscopy texture and the diffraction patterns. A crystalline phase is observed at even higher ϕ_s.

The overall ternary phase diagram at 30 °C is shown in Figure 15.

Discussion

The high viscosity of the isotropic phase at low values of α is consistent with formation of wormlike micelles. This behavior is very similar to that seen in mixtures of CTAB with salts such as KBr, sodium salicylate, and sodium tosylate.[2,18,19] The growth of these long flexible

(18) Khatory, A.; Lequeux, F.; Kern, F.; Candau, S. J. *Langmuir* **1993**, *9*, 1456.

micelles is attributed to the decrease in the spontaneous curvature of the CTAB micelles in the presence of these salts.

The observation of a lamellar phase over an extended range of ϕ_s around $\alpha \approx 1.0$ is reminiscent of the behavior of mixtures of cationic and anionic surfactants[6−8] and also of some mixtures of cationic surfactants and anionic drugs.[20] Although the HN^- counterion is much shorter (length ≈ 5 Å) than the CTAB molecule (length ≈ 17 Å), its incorporation in the CTAB micelle seems to have a similar effect as that of a much longer anionic surfactant. The diffuse peaks in the diffraction patterns of the L_α^D phase at lower values of ϕ_s occur in a direction normal to the lamellar peaks and can be attributed to positional correlations between defects lying in the plane of the bilayer (Figure 9). Consistent with this picture, the bilayer thickness estimated from the observed lamellar spacing and the surfactant volume fraction is about 10% lower than that obtained at high ϕ_s when the diffuse peak is absent. Such diffuse reflections have been observed in the lamellar phase of some surfactant systems, such as cesium pentadecafluorooctanoate (CsPFO).[21] Small angle neutron scattering as well as water diffusion experiments have shown that the diffuse reflections arise from water-filled pores in the bilayer.[22] These defects heal on adding $CsCl_2$ or increasing the surfactant concentration to form a lamellar phase without defects. Such curvature defects are also found in some mixed-surfactant systems.[23] Neutron scattering studies on the SDS−alcohol−water system have shown that the number of defects per unit area increases as the SDS/alcohol ratio increases. However, the pores disappear gradually when the water content is decreased. The existence of similar curvature defects has also been proposed in mixtures of dimyristoylphosphatidylcholine (DMPC) with a shorter chain lipid dihexanoylphosphatidylcholine (DHPC).[24] The diffraction patterns of this system do not show any diffuse peaks, and the presence of these defects is deduced from the fact that the observed lamellar periodicity is much less than that estimated from the lipid volume fraction. The absence of positional correlations between the defects in this case might be due to the fact that they are quasi-circular pores with no well-defined size. On the other hand, in systems where the diffuse peak is seen it may be better to envisage the bilayers as a meshlike structure with ribbonlike segments rather than as a continuous sheet littered with porelike defects. Unlike in the CsPFO−water system, the spacing corresponding to the diffuse peak in the present system increases with increasing ϕ_s (Table 2). Presently it is not clear if this difference is critical for the occurrence of the intermediate phase in the latter.

The formation of these curvature defects has been explained in terms of the tendency of one of the surfactant species to aggregate into spherical or cylindrical micelles, both of which have high positive values of mean curvature. The microenvironment in the edge of these defects is very similar to that in the micelles, and hence, their formation helps to reduce the overall energy of the system.[25] A single ionic surfactant can also mimic a two-component system by having a higher degree of ionization near the edges of these defects. In the present case it is very likely that the CTAB concentration is higher near the defect edges, reflecting the preference of CTAB to form cylindrical micelles. The curvature defects in the lamellar phase gradually disappear on decreasing the water content at high temperatures. However, at lower temperatures an intermediate phase occurs between the two lamellar structures. This phase is found over a very broad composition range $0.25 \le \alpha \le 1.5$. Microscopy observations suggest that this phase is optically uniaxial, but further work is under way to establish its structure.

On increasing α to 1.85 the lamellar phase disappears and the phase behavior is somewhat analogous to that at very low values of α. A similar behavior is also seen in other mixtures of CTAB with strongly bound hydrophobic counterions and is usually attributed to the fact that the aggregates at these compositions are highly charged, as those at very low counterion concentration. The only difference is the observation of the nematic phase at $\alpha = 1.85$. In this connection it should be noted that a nematic phase made up of rodlike micelles has been reported in the CTAB−water system from 26 to 30 wt % CTAB concentration below 42 °C.[11] However, we did not observe this phase even at the lowest α studied. The nematic phase seems to be suppressed by SHN at these compositions, although at much higher values of α this phase reappears. The flow alignment of the nematic phase, observed in the diffraction experiments, and the absence of pseudo-isotropic regions in its microscope texture suggest that it is made up of linear surfactant aggregates. The high viscosity of this phase indicates that these are long wormlike micelles and not shorter rodlike ones proposed in the N phase of the binary CTAB−water system.

The overall symmetry of the ternary phase diagram about the equimolar composition of the two species is very similar to that observed in the case of mixtures of cationic and anionic surfactants.

Conclusion

A partial phase diagram of the CTAB−SHN−water system has been constructed from optical microscopy and X-ray diffraction studies. A variety of phases, such as hexagonal, lamellar with curvature defects, intermediate, regular lamellar, and nematic, have been identified. The phase behavior is found to be fairly symmetric about the equimolar CTAB−SHN composition, as seen in mixtures of cationic and anionic surfactants. The curvature defects, present in the L_α^D phase at higher water content, are gradually annealed on decreasing the water content at high temperatures. However, at lower temperatures this occurs across an intermediate phase, which most probably consists of an ordered array of such defects and is the subject of ongoing investigations.

Acknowledgment. We thank H. N. Shreenivasa Murthy for his help in preparation of SHN and M. Mani for technical assistance.

LA051781Q

(19) Hartmann, V.; Cressely, R. *J. Phys II Fr.* **1997**, *7*, 1087.
(20) Bramer, T.; Paulsson, M.; Edwards, K.; Edsman, K. *Pharm. Res.* **2003**, *20*, 1661.
(21) Lever, M. S.; Holmes, M. C. *J. Phys. II Fr.* **1993**, *3*, 105.
(22) Holmes, M. S.; Sotta, P.; Hendrikx, Y.; Deloche, B. *J. Phys. II Fr.* **1993**, *3*, 1735.
(23) Hendrikx, Y.; Charvolin, J.; Kekicheff, P.; Roth, M. *Liq. Cryst.* **1987**, *2*, 677.
(24) Nieh, M.; Glinka, C. J.; Kroeger, S.; Prosser, R. S.; Katsaras, J. *Langmuir* **2001**, *17*, 2629.
(25) Bagdassarian, C. K.; Roux, D.; Benshaul, A.; Gelbert, W. M. *J. Chem. Phys.* **1991**, *94*, 3030.
(26) Holmes, M. C. *Curr. Opin. Colloid Interface Sci.* **1998**, *3*, 485.
(27) Kekicheff, P.; Cabane, B. *J. Phys.* **1987**, *48*, 1571.
(28) Kekicheff, P.; Tiddy, G. J. T. *J. Phys. Chem.* **1989**, *93*, 2520.
(29) Funari, S. S.; Rapp, G. *Proc. Natl. Acad. Sci. U.S.A.* **1999**, *96*, 7756.
(30) Hendrikx, Y.; Charvolin, J. *Liq. Cryst.* **1992**, *3*, 265.
(31) Funari, S. S.; Holmes, M. C.; Tiddy, G. J. T. *J. Phys. Chem.* **1992**, *96*, 1102.
(32) Funari, S. S.; Holmes, M. C.; Tiddy, G. J. T. *J. Phys. Chem.* **1994**, *98*, 3105.